Available online at www.sciencedirect.com
SCIENCE DIRECT®
International Journal of Mass Spectrometry 235 (2004) 243–253
International Journal of Mass Spectrometry
www.elsevier.com/locate/ijms

A modular data and control system to improve sensitivity, selectivity, speed of analysis, ease of use, and transient duration in an external source FTICR-MS

T.H. Mize, I. Taban, M. Duursma, M. Seynen, M. Konijnenburg, A. Vijftigschild, C.V. Doornik, G.V. Rooij[1], R.M.A. Heeren*

FOM Institute for Atomic and Molecular Physics, Kruislaan 407, 1098 SJ Amsterdam, The Netherlands

Received 18 March 2004; accepted 7 May 2004

Abstract

We present here a new Fourier transform ion cyclotron resonance mass spectrometry (FTICR-MS) controller designed and constructed to meet the growing need for increased speed, memory, and ease of use. The system realizes these goals via the first published application of fast PXI bus technology and by employing a graphical user interface (GUI) for control of all aspects of ion production, delivery, containment, manipulation of internal and kinetic energies, and measurement in an external source instrument. Additionally, new hardware for monitoring and control of these aspects and for processing extended datasets both to and from the instrument have been implemented.

The modular nature of the control hardware makes the instrument platform, in this case a modified external source 7T FTICR-MS, irrelevant. The GUI consists of two separate modules; one provides a temporal representation of the pulses, voltages (rf and dc), and dc heater currents that control all aspects of the experiment while the other provides complex data analysis capabilities and design of excitation waveforms. Real-time monitoring of the transient signal is available in this module as well as near real-time monitoring of the resulting mass spectrum (using a truncated dataset). A PXI bus with 40 digital to analog converters (DAC) and 64 digital (TTL) sources drive the source, optics, and trapping functions of the instrument as well as the other peripheral hardware. Acquisition is realized using a VME bus with a TTL triggered program resident on an embedded processor to minimize dead time. The acquisition system is equipped with 192 MB memory for both excitation and detection waveforms with FIFO buffering to provide full rate bandwidth of 10 MHz, and four digital down converters (DDCs) to enable mixing of heterodyne signals for narrow band measurements completes the ensemble.
© 2004 Elsevier B.V. All rights reserved.

Keywords: FTMS; Modular data station; Ion cyclotron resonance; Excitation; Stored waveform inverse fourier transform; Graphical user interface; Ion isolation

1. Introduction

It is the nature and, indeed, a necessity of the experimental sciences that the reach of the scientist exceeds the capabilities of the instrumentation. The explosive growth of Fourier transform ion cyclotron resonance mass spectrometry (FTICR-MS) [1,2] yields a prime example of how quickly the instrumental control technology is rendered obsolete by the expanding needs of users. FTICR-MS provides a host of analytical capabilities unavailable in other instrumentation. Ions of high m/z can be trapped and measured with unprecedented resolution and mass accuracy, and can be manipulated by a variety of gas phase chemical (ion-molecule chemistry, electron absorption, photochemistry) and physical (surface and collision induced dissociation, etc.) means.

Still, this powerful family of instrumentation has yet to reach its full theoretical limits. For instance, the thermal cyclotron radius of the ions and the rate of magnetron radial diffusion determine the high m/z limit for a given magnetic field strength and trapping potential [3,4]. At 7 T and 1 V trapping potential, the upper limit should be ~138 kDa and the practical limit—i.e., the highest m/z with thermal radius small enough to allow excitation and detection around

* Corresponding author. Tel.: +31 20 608 1234; fax: +31 20 668 4106.
E-mail address: heeren@amolf.nl (R.M.A. Heeren).
[1] Current adress: FOM Institute "Rijnhuizen", Edisonbaan 14, 3439MN Nieuwegein, The Netherlands.

1387-3806/$ – see front matter © 2004 Elsevier B.V. All rights reserved.
doi:10.1016/j.ijms.2004.05.003

70 kDa [5]; but, this theoretical limit is further attenuated by limited control of the ion population size and the inability to exploit low trapping potentials. Regardless, many of these limiting parameters' effects can be minimized by improved instrument temporal and electronics control [5,6].

Despite the high performance an FTICR-MS data system is surprisingly simple, minimally requiring a mechanism for time-dependent assignment of a few dc and rf voltages, TTL (or other) pulses (with ~1μs resolution), and a method of rapidly digitizing the resultant image current. This is more than mere conceptual simplicity, however, as Beu and Laude demonstrated by successfully implementing an FTICR-MS employing the bare minimum of off-the-shelf components including only a frequency synthesizer, a delay pulse generator, a broadband rf amplifier, a signal preamplifier, a fast transient digitizer, and a personal computer (with a 286 processor) to coordinate the electronic devices and to process and analyze the data [7]. But, this simplicity is complicated by the large number of control parameters that must be available for manipulation by the operator in order to maximally exploit the capabilities inherent in a given system; consequently, user interfaces have taken a variety of formats [7–11]. As a series of timed pulses, this experiment translates well graphically to a timeline of events that are easily understandable by even the novice user with no degradation of control for the expert. Several prior non-commercial PC-based modular systems have been presented in the past, notably MIDAS [10], which is still in general use and employed to great effect by both short term visitors and permanent staff at NHMFL and several other laboratories [10].

Stored waveform inverse fourier transform (SWIFT) [12] excitation further facilitates ion selection and excitation with rf excitation tailored to highly specific ranges of frequencies and applied powers by transforming the desired frequency domain excitation into the corresponding time domain pulses while distributing the required excitation power across the duration of the pulse. The complexity of the SWIFT algorithm's output makes the use of programmable waveform generators critical to their application. Large blocks of memory are required for storage of the long duration pulses constructed to isolate a given ion or range of ions. An MS^n experiment will require *n* such waveforms to be loaded and ready for instant translation to the cell excitation plates via digital-to-analog converters DACs. Past solutions to SWIFT application have used static memory banks of 16 kword to 1 Mword, DAC with a precision of typically 8–12-bit, and sample rates from 1 to 20 MHz (corresponding to Nyquist limited output frequencies of 0.5–10 MHz). The size of SWIFT waveforms, often several Mwords requiring several seconds of upload time, can limit the applicability of multiple pulses in a single experiment. Our arbitrary waveform generator (AWG) system overcomes such limitations via dual-use, on-board memory of 192 MB.

Limitations on the size of acquisition memory can also limit the bandwidth (or rate) of digitization which is determined by the highest cyclotron frequency (and therefore lowest *m*/*z*) of interest in the experiment. That is, the size of memory allocation for a given transient is determined by the mass range with rate of digitization corresponding to the lower *m*/*z* and the required duration of the transient defined by the desired high *m*/*z* resolution. Given sufficient memory, allocation becomes a moot point and a series of experiments can be performed and the signals recorded with no breaks between experiments to transfer the data from digitizer to PC. That is, the experiment duty cycle becomes simply a function of the duration of any single experiment in the series.

Bearing these parameters in mind, we present here the development of a combination of modular components to serve as an easily expandable data system and hardware controller for FTICR-MS. The system consists of a PC-resident graphical user interface (GUI) for design of pulse sequences and initiation of experiments, a PXI rack loaded with DAC and TTL boards to provide analog and digital control pulses with sub-microsecond timing accuracy, and a new arbitrary waveform generator developed for both the excitation and detection of ion motions in the FTICR cell. The generator contains 192 MB RAM for the combined storage of excitation waveforms and detected image current. A local processor at the hardware interface that is triggered by the PC after the control waveform is loaded assures real-time instrument control. Additionally, the system takes advantage of the improved ion transmission, selection, and storage capabilities of quadrupole ion optics with microsecond bias control provided by the PXI box.

In this paper, we present the details of the graphical user interface, the in-house designed electronics and the functionality of the in-house developed software. The performance of the AWG system is demonstrated with FTICR-MS measurements. The results of isolating a number of components of a synthetic polymer molecular weight distribution by simultaneous ejection of all other components and the isolation of a multiply charged protein isotope illustrate the versatility and frequency selectivity of the system while the presentation of high *m*/*z* species provide a measure of the support hardware control capabilities.

2. Materials and methods

2.1. Software

The AWG and "arbitrary waveform editor"(AWE) software is written in C++, using Microsoft Visual Studio Net 2003. The software uses some external libraries for hardware control, user interfacing and mathematical functions. The programs are developed using object-oriented techniques. Since the programs share a common need for particular data types and must be able to exchange data, a library is created to host the common classes and functions.

AWG is the pulse designing backbone of the system, controlling all the hardware timing and levels. It provides the

Table 1
The ranges of values of the various controllable elements in the experiments we perform; however, the system is easily expandable

Ion source		rf ion guides	
Spray tip	±5000 V	Q1 bias	±25 V
Capillary	±400 V	Q2 bias	±25 V
Capillary heater	0–5 A	rf "power"	0–5000 V
Tube lens	±400 V	Gate voltage 1	±100
Skimmer	±100 V	Gate voltage 2	±100 V
Qbias, source	±25 V	End plate	±25 V
Extraction Lens	±25 V	Gas valve 1	TTL
Conduction limit	±25 V	Gas valve 2	TTL
		Gate valve	TTL
Cell		External equipment	
Trap electrode 1	±100 V	Pyrolysis power supply	TTL
Trap electrode 2	±100 V	QEA relay	TTL
EV 1	±25	MALDI laser	TTL
EV 2A	±25 V	Polarity switch, capillary	TTL
EV 2B	±25 V	Polarity switch, tube lens	TTL
Cell heater	0–5 A		
Filament heater	0–5 A		
Electron energy	±100 V		

user-interface and stores/retrieves all data required to do FTICR-MS measurements. It runs on the Microsoft™ Windows 2000 platform and thus creates a familiar and intuitive environment for novice users. The mapping of the various analog and digital output signals to the hardware, the output range, name and type of signal is defined in a configuration file (INI). This allows the user to easily change or add signals to the system without the need to change the source code of the software. The signals can be grouped together to give the user a better understanding of their function; some of the groups are typically: ion source, ion optics, cell, and external equipment. Signal ranges are shown in Table 1.

The GUI provides various tabbed pages that display either the static state of the output signals or the temporal dependence of the signals. In the "static" page all signals are visible per group and ready for real-time adjustment for tuning purposes. All static parameters can also be made time-dependent on this page, in which case the "static" value is the initial state of the corresponding hardware. The actual voltage of a signal can be read back both during and between experiments to check for faults, leaks or shorts in the system. In the time-dependent view mode (also refered to as "sequence" view) all non-static signals are shown in a graphic timeline. This timeline gives a rapid insight into the sequence of events during a measurement.

Apart from the analog and digital output signals there is a special signal called "AWG/transient digitization"(AWG/TD) for the excitation and detection of the ions in the cell. On this signal one or more excitation pulses or combined excitation and transient detections can be inserted. The excitation pulses are loaded to the AWG system prior to sequence execution. Also memory for the detected transients is allocated up to the full 192 MB memory. In fact, during an experiment, the actual transient signal at the detector plates can be visualized as well as the FFT frequency- and mass-domain data of a limited subset of the time-domain data (for instance, the first 64k data points) can be monitored within the GUI for approximately real-time spectral visualization during the measurements.

All experiments are stored on the local hard disk or on a high capacity network drive. Besides the transient data, the whole measurement configuration and sequence is saved to disk and an entry is made in a database. In the database information about the sample, the experimentalist's name, source parameters, external equipment used, project name and comments are stored. This database allows for easily searching and indexing experiments, retrieving their settings and/or viewing the results.

The AWE has two important mass spectral data processing functions. First, AWE can be used to inspect and postprocess raw FTICR data. Information on peak properties (m/z, frequency, charge state, intensity and resolution in both power and magnitude modes, and the Fourier limited resolution) are readily available. Secondly, AWE is used to design excitation waveforms for use in AWG. Simple interfaces are employed to specify resonant and sustained off-resonance (SORI) sine wave excite pulses while either a measured or calculated transient can be used to create a template for SWIFT pulse design. In principle, any arbitrary excitation waveform that fits in the memory allocation can be loaded.

Each mass spectrum and generated excitation waveform has four display modes: raw transient and frequency, power, and magnitude spectra. The template mass spectrum is capable of automatic peak picking and calibrated to match the machine constants. In a typical SWIFT experiment, the template transient signal is loaded into AWE and its relevant measurement parameters (bandwidth for the excitation, the size of the dataset, and the calibration constants, for

instance) loaded into the SWIFT calculation variables. The desired excitation profile—its power spectrum—is then constructed graphically as an overlay directly on the template mass spectrum; the software simultaneously smoothes the Gibbs oscillations by application of a window convolution algorithm in the corresponding frequency domain spectrum. This smoothed spectrum is used to calculate the quadratic phase versus frequency function for an optimal spread of the excitation power in the SWIFT waveform [13]. Inverse Fourier transformation of the magnitude and phase spectra yields the SWIFT excitation (time-domain) waveform.

The uniformity of the excitation spectrum amplitude produced is, particularly in the case of SWIFT waveforms, a function of the accuracy of the digital-to-analog conversion [14]. It is therefore advantageous for the maximum amplitude of the waveform to correspond with the dynamic range of the DAC. In general, this is automatically achieved in the calculation of the optimal phase function according to the SWIFT algorithm [15,16]. The associated hardware settings are attached in a header and the waveforms stored to disk. Upon use in the AWG software, the waveforms are normalized to maximally use the full range of the 12-bit DACs.

In addition to the SWIFT waveforms, it is also possible to create the traditional time-domain excitation waveforms such as frequency sweeps (for broad band excitation) and single frequency sine waves are available to facilitate both resonant and off-resonant (SORI) [17,18] MS^n experiments. Although not currently integral to the software, any arbitrary function the user can imagine, such as correlated harmonic excitation fields (CHEF), [19,20] can also be uploaded

The system's flexibility in constructing the most versatile experiments is illustrated in the sample AWG sequence that is depicted in Fig. 1, a sequence screen shot of the GUI. Its practical relevance is that it contains all excitation events that are required for FTICR-MS experiments in which electron capture dissociation (ECD) and subsequent SORI dissociation of ions is achieved. Briefly, this MS^3 experiment entails collisional cooling of the introduced ion distribution, the SWIFT isolation of the precursor ions, introduction of low energy electrons (ECD), a small reaction/cooling delay,

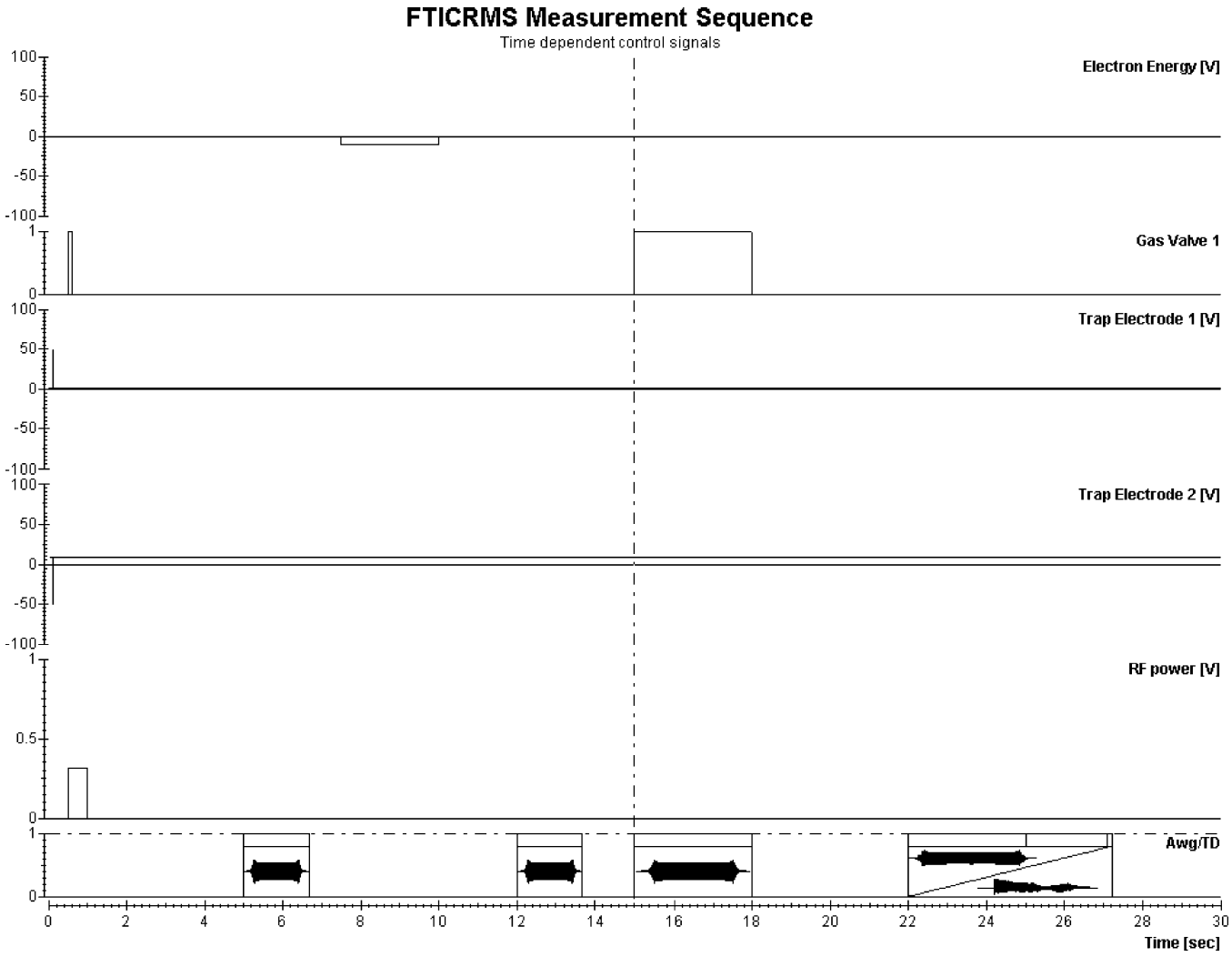

Fig. 1. GUI sequence shot from AWG software.

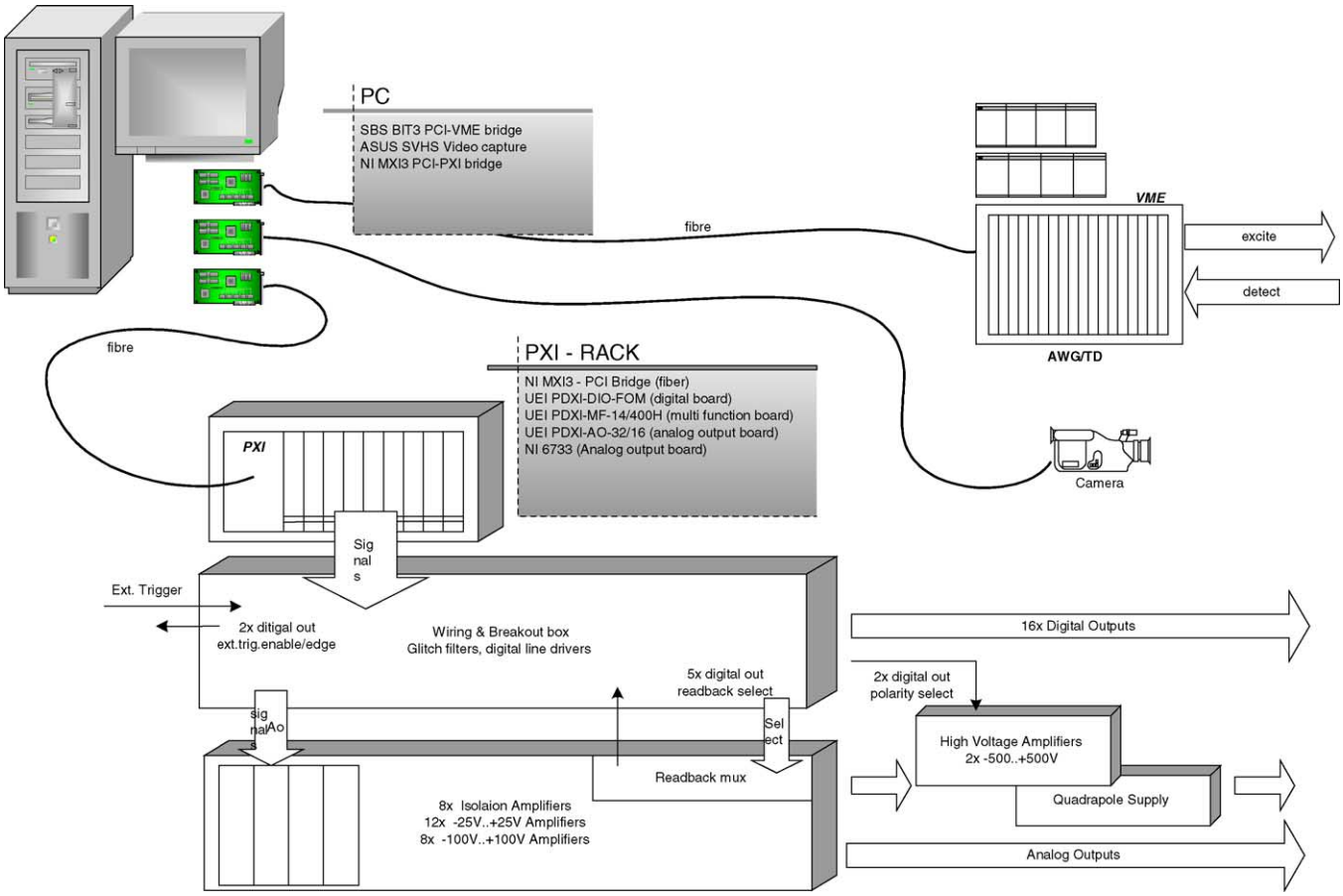

Fig. 2. Block diagram of the FTICR-MS controller.

the second SWIFT isolation, SORI dissociation of one of the ECD products, a pumping delay, and finally broadband excitation to produce a detectable signal for all remaining ions. Additionally, the sequence can be repeated several times, using inner summation-scan loops, or outer serial-scan loops, or both. The inner loop is used to perform experiments in which the results of several scans are co-added, improving the S/N ratio by up to $n^{1/2}$. The outer loop is used to produce a series of experiments in which one or more parameters of the sequence can be changed at the start of each loop. The target parameters can be varied according to feedback in the form of signal values, loop numbers, and/or analog inputs. This means that any pulse duration, signal level, static value, or certain excite/detect values can be varied in a flexible and automated way. For example, serial measurements can be automatically taken each with a different rf-power output (or any other parameter), increasing from 0 to 100% of the full range.

2.2. Hardware

The FTICR-MS experiments were performed on a 7 T external source FTICR-MS that has evolved beyond recognition from its original commercial platform. The development of the instrumental layout and experimental procedures are described in detail elsewhere [21–23]. Briefly, the instrument uses a homebuilt electrospray ionization source, three quadrupole rf ion guides to transfer ions over four stages of differential pumping, and an elongated and thermostated (temperature control from 77 to 438 K) open cylindrical cell [24].

The electronics and computer hardware of the FTICR-MS experiment consists of a PC host system, a PXI chassis with several commercially available data-acquisition boards, a VME system and a few racks of signal amplifiers with various output levels. The host system is an Intel Pentium™ 4 based computer with 1.8 GB RAM, two fiber-optic communications boards, one National Instruments MXI-3 interface to the PXI chassis, and one SBS Bit3 PCI-VME model 620 bridge to the VME crate. Furthermore it has a CCD camera and video adapter with a video-input supplying close up images of the spray needle within the AWG control program. A schematic of the hardware layout can be seen in Fig. 2.

The control boards in the PXI-chassis (all acquired from United Electronics Industries, Canton, MA 02021) provide all analog signals, digital outputs and triggers, as well as the analog inputs for the read back. The system consists of one digital I/O board which is specially adapted for use as a time frame generator (TFG) card (PDXI-DIO-64ST -FOM), a 400 kHz 14-bit multifunction board (PDXI-MF-14/400H),

and an analog output board (PDXI-AO-32/16). The TFG has 64 programmable outputs with a time resolution of 50 ns and an approximate accuracy of 100 ns. The length of the time frame is made independent of the onboard memory by streaming DMA from the PC main memory. The multi-function board is used for read back of the static signals levels as well as sampling during experiments. The analog output board has 32 channels of 16-bit DACs. The TFG card generates the triggers and digital signals according to the timing defined in the sequence of the AWE program. It triggers the DACs to generate steps, pulses and ramps; additionally, it triggers the MF-board sampling. A step requires a single trigger, a pulse (essentially a special case of two steps) requires two triggers, and ramp requires continuous triggering. Depending on the type and configuration of the output board it either uses one trigger to update all output channels or one trigger to update a single channel. Additionally, a National Instruments (11500 North Mopac Expressway, Austin, TX 78759) NI-6733 analog output board was inserted to the PXI chassis to complete the setup with another 8 channels of 16-bit DACs that have better output specifications than those on the UEI board.

All analog outputs are configured for ±10 V and amplifiers boost the signals to their appropriate levels, either ±25 V or ±100 V. A limited number of isolation amplifiers are employed with gain 1× to buffer the rf-power supplies and the high voltage modules.

The VME crate houses our home built AWG/TD system and has 192 MB of memory (3 times 64 MB, Chryslin Industries Inc., Westlake Village, CA) to store both excitation pulses and transient signals. The excite generator (AWG/TD) has a maximum output frequency of 20 MHz and 12-bit resolution and an attenuation circuit to adjust the output power without compromising DAC resolution. The excitation signal is calculated so that the highest amplitude in the signal matches the highest possible amplitude of the DAC in order to increase the accuracy in the analog output. This full-scale signal is then passed to a summing step attenuator with steps of 4.01, 8.02, 15.41, and a 31.82 dB (0 dB achieved with no steps active, ∼64 dB with all active). This signal is further passed through a reference DAC that can further attenuate from 0 to 6 dB in 256 steps yielding a full range from 0 to 70 dB with high precision. The transient digitizer (TD) has an analog-to-digital converter with 12-bit resolution and maximum sampling frequency of 20 MHz (10 MHz in summation mode). The data can be reduced with an adjustable finite impulse response (FIR) low pass filter within the range 312.5 kHz down to 153 Hz; alternatively, up to four simultaneous narrowband spectra can be measured with the digital down converters (DDCs) bandwidth up to 315 kHz.

The transient is written to and retrieved from the memories based on the measurement type: Wideband TD mode (16 bit), Wideband TD-SUM mode (32 bit), Narrowband TD (NBTD) mode (real part 16 bit, imaginary part 16 bit), and Narrowband TD-SUM (NBTD-SUM) mode (real part 32 bit, imaginary part 32 bit). To maintain unchaperoned VME control of the excitation and detection in these experiments, bandwidth is sacrificed in direct proportion to the size of the various data structures. To be more specific, in TD mode two 16 bit data points are combined to make a 32 bit word to be written to memory at the full 10 MHz bandwidth. TD-SUM mode; the mode in which consecutive transients are continuously co-added in memory requires a simultaneous read back of the previous data and a read of the new data to be combined, thus reducing the maximum data rate by a factor of two to 5 MHz; NBTD mode requires a read of the synthesized mixer signal and the incoming raw data, similarly reducing the write speed to 5 MHz. A similar argument as for TD-SUM mode demonstrates that the maximum bandwidth in NBTD-SUM mode is 1/4 the full rate, or 2.5 MHz.

The output of the VME system is connected to the FTICR-MS instrument, where it is amplified and split into two 180° out-of-phase channels to drive the excitation plates of the ICR analyzer cell. Alternatively, the splitter can be shunted so that a two-plate, pseudo-quadrupolar field can be delivered making realization of the quadrupolar excitation-axialization (QEA) experiment possible.

2.3. Reagents

Cytochrome C from bovine heart was measured by means of ESI-MS and was purchased from Aldrich (Milwaukee, WI). Cytochrome C was sprayed from a ∼25 μM solution with a solvent composition of 49:49:2 MeOH:H_2O:HAc. Linear polypropylene glycol (Mw ≈ 750) was obtained from Sigma-Aldrich (St. Louis, MO) and dissolved in 50% (v/v) aqueous MeOH plus 0.05% trifluoroacetic acid to 50 μM in a glass vial. Sodium and potassium ions were already present in the polymer or the container, and cesium ions derived from an incompletely cleaned electrospray capillary.

3. Results

Fig. 3 illustrates the ion selection capability of the AWG/AWE controller. The polypropylene glycol spectrum shown in Fig. 3A) was used to design a SWIFT pulse for the simultaneous isolation of the monoisotopic sodiated peak of each oligomer from $n = 10$ to 15. The SWIFT template was generated with notches (and, therefore, no net excitation) around the target peaks while regions of full excitation (and thus ejection) around the other ionic species formed by adduction of either a proton or one of the other alkali metals (potassium or cesium), as seen in the insert. After application of the isolation waveform, only the target species remain (Fig. 3B).

The frequency selectivity in AWG excitation events was investigated in more detail on Cytochrome C. The mass spectrum recorded by broadband excitation is shown in Fig. 4A. The inset in Fig. 4A is an expansion of the mass scale around the 15+ charge state which shows that the mass

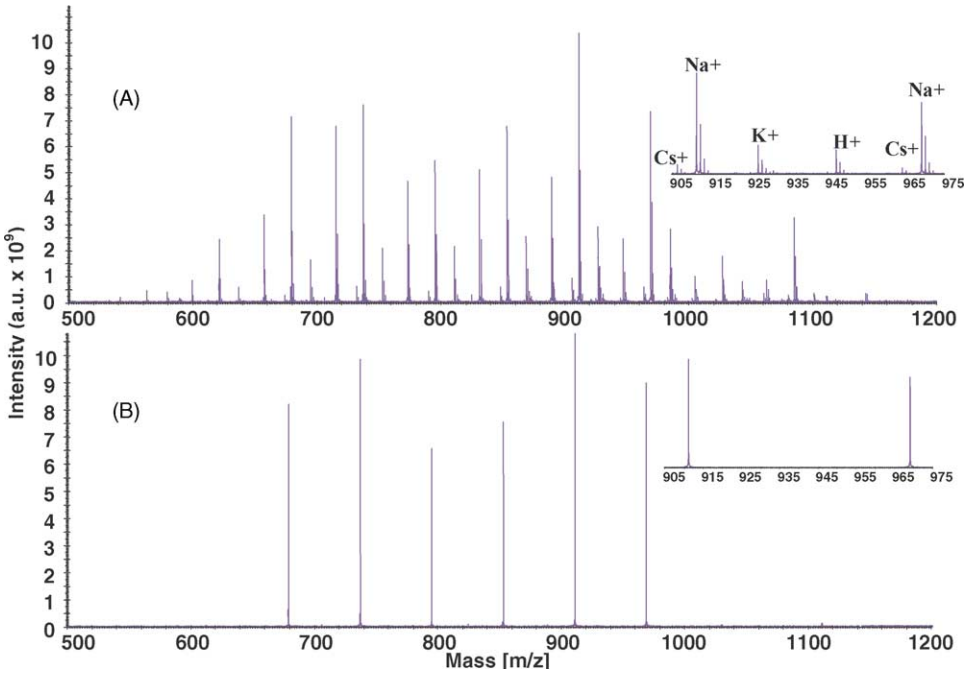

Fig. 3. ESI-FTICR-MS spectra of linear polypropylene glycol. (A) The entire distribution including $M + H^+$, $M + Na^+$, $M + K^+$, and $M + Cs^+$ species, (details in inset). (B) Same distribution following isolation of only the monoisotopic sodiated species.

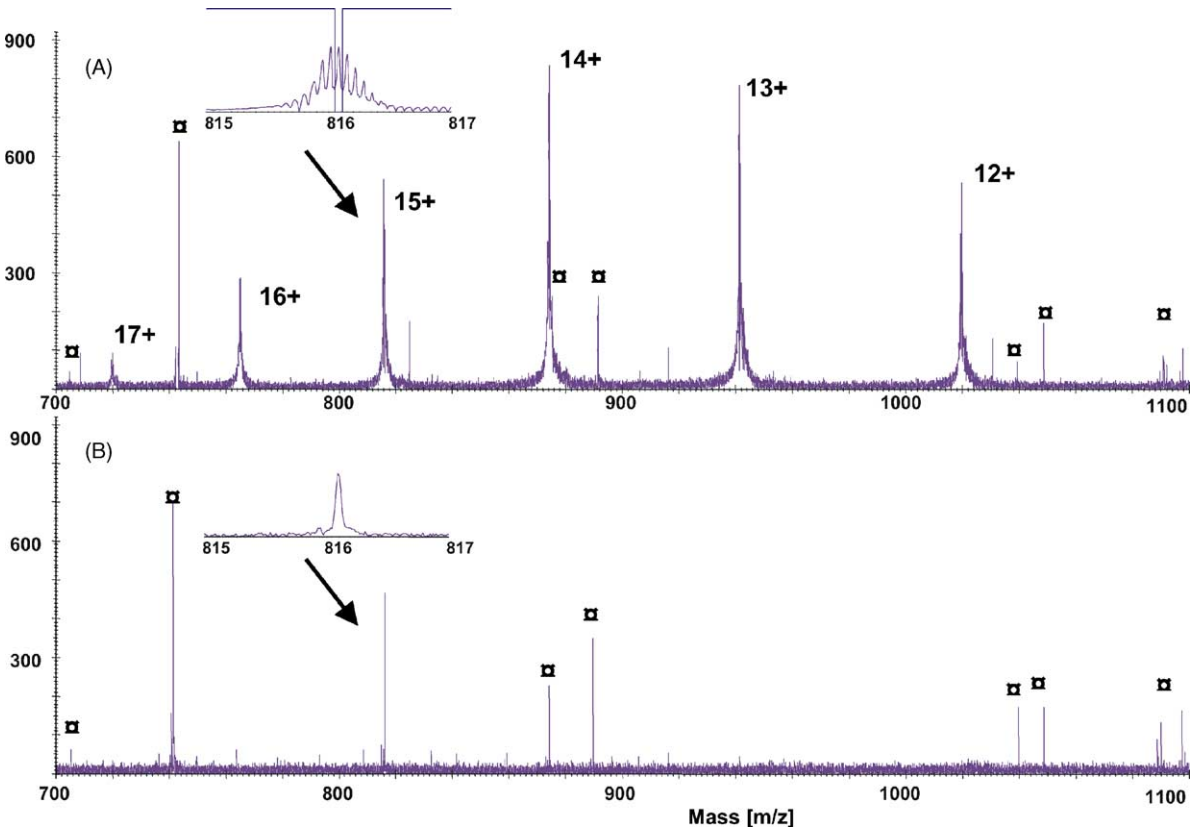

Fig. 4. Single isotope isolation from 15+ charge state of Cytochrome C. Peaks labeled with a ¤ denote rf noise peaks

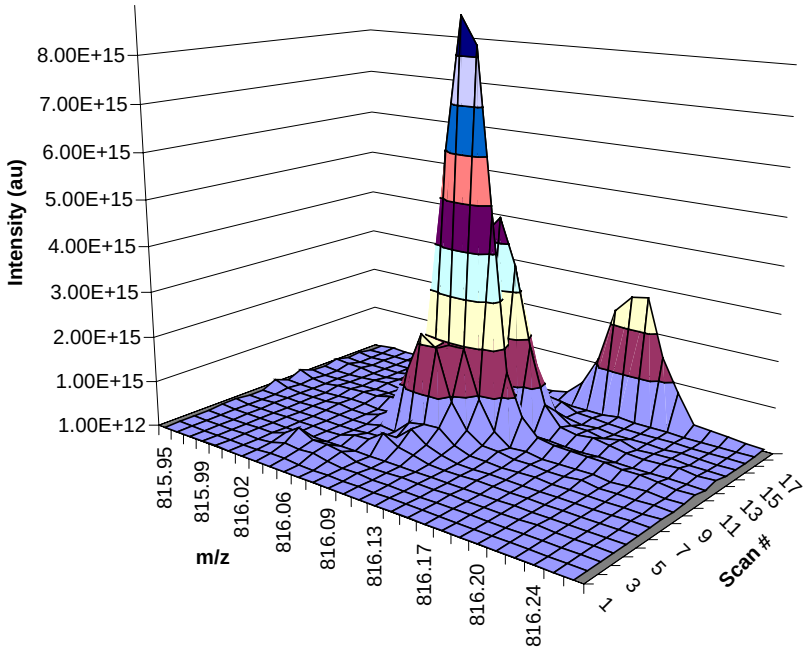

Fig. 5. Series of mass spectra taken to measure the frequency selectivity of the SWIFT pulse. The center of the retention window in the SWIFT design was shifted in 0.01 Da steps from 816.0450 to 816.1650 *m/z* showing that the falloff from maximum to 50% signal intensity occurs in ∼1.6 Hz implying a frequency selectivity of ∼3.2 Hz.

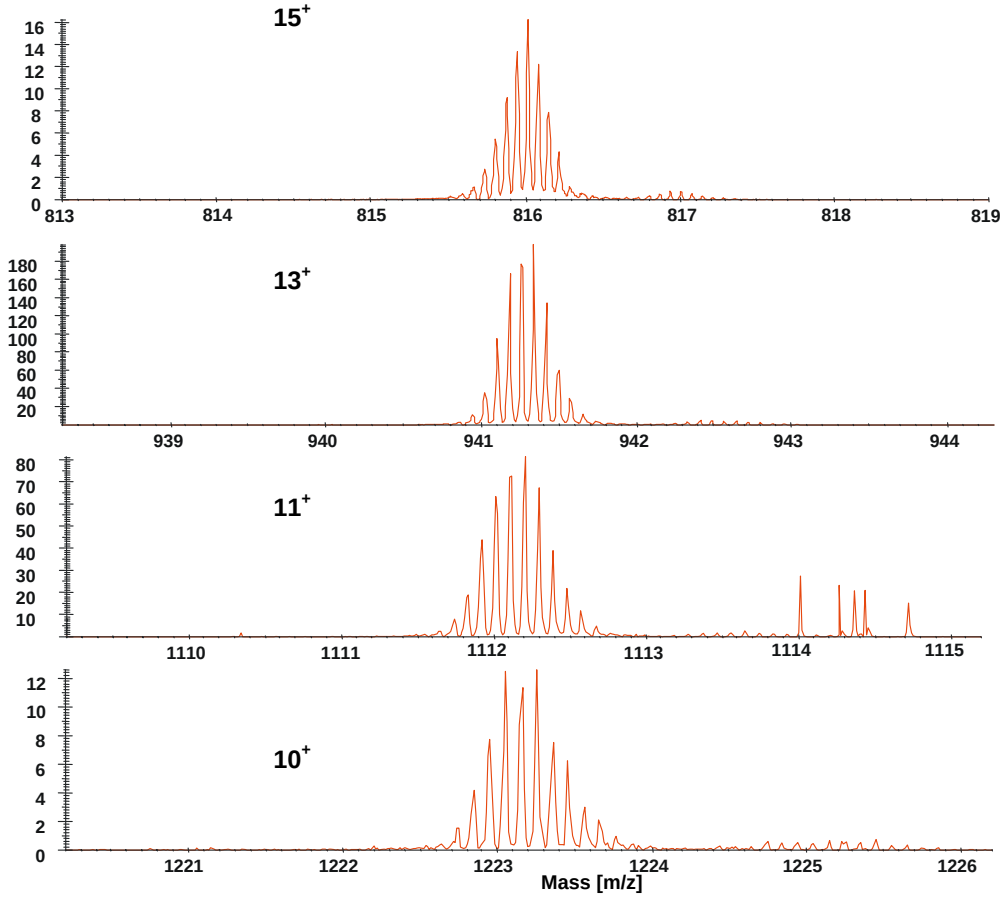

Fig. 6. Four simultaneously collected, 8k point, heterodyne measurements with mixer frequency of 4 kHz showing the advantages of increased signal duration and digital filtering.

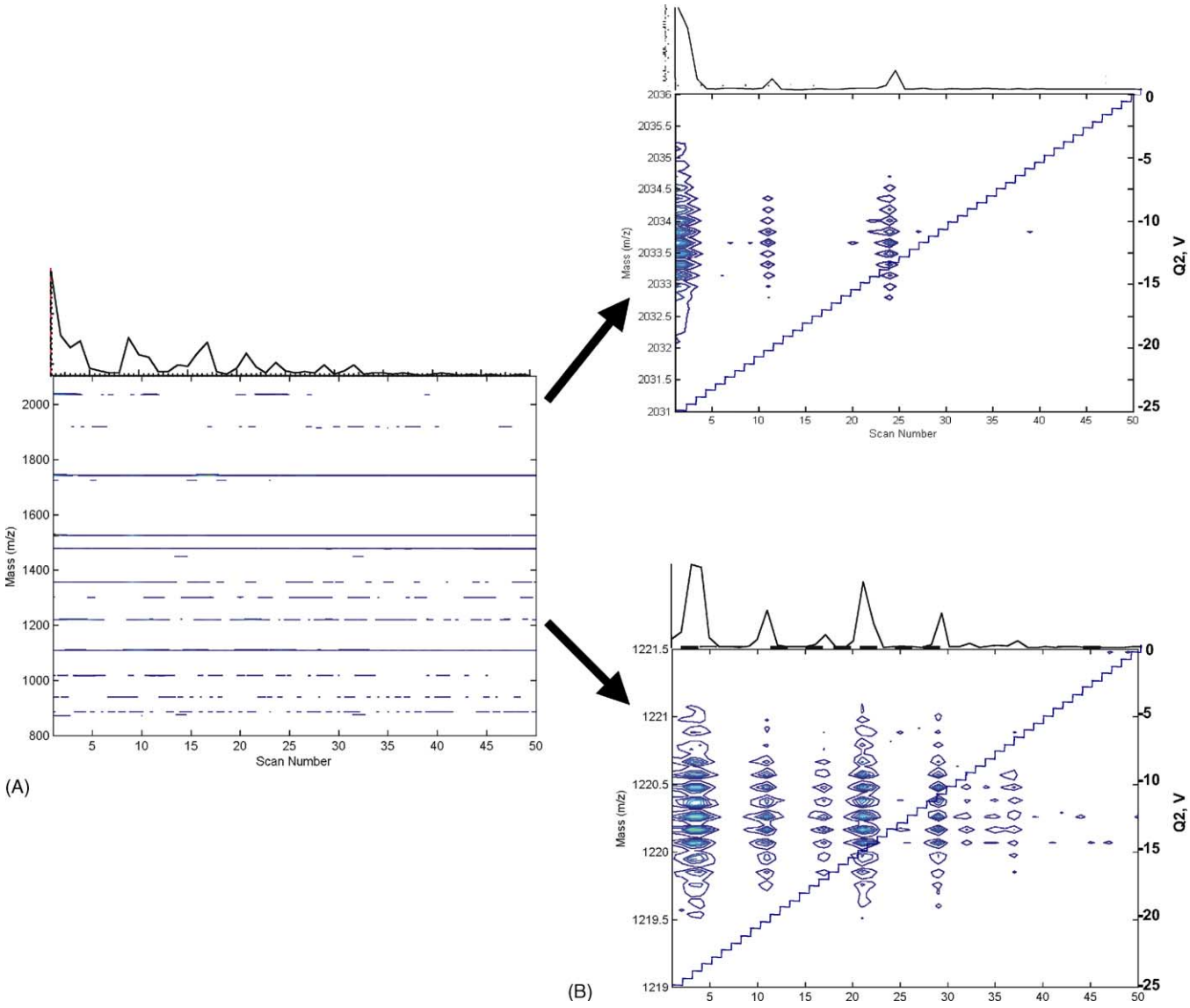

Fig. 7. Two-dimensional mass spectra obtained at 2.5 s duty cycle while scanning through bias voltage on the final source quadrupole. (A) The total and selected ion currents are shown above the full mass spectra and (B) selected mass range spectra, respectively. The quadrupole bias voltage is shown as an overlay on the selected ion spectra for clarity.

resolution (here, $m/\Delta m_{50\%} = 37100$ at m/z 816.09) is sufficient to resolve the ^{12}C and ^{13}C isotope peaks for the individual charge states. The number of isotope peaks appearing within a single mass unit was determined to identify the number of charges on the ion [25]. In this way it was found that the charge state distribution in Fig. 4A ranges between12+ (around m/z 1019.8) and 17+ (around m/z 720.1).

The expanded mass scale also reveals the close isotope spacing for the 15^+ charge state. The difference in m/z ratio between adjacent isotope peaks in this charge state is equal to 0.067 u. This corresponds to cyclotron frequency differences of less than 11 Hz at an average cyclotron frequency of 131.6 kHz. Isolation of a single isotope peak from this cluster is evidently challenging and an excellent test for the system's frequency selectivity. This was achieved by tailoring a 1 Mword broad band SWIFT waveform to eject all ions from $461.85 < m/z < 816.06$ and from $816.15 < m/z < 2558.20$ and to leave ions from $816.06 < m/z < 816.15$ unaffected. The transform of the SWIFT pulse back to magnitude mode mass-domain is shown as an overlay on the inset. It reveals the high resolution of the mass notch at m/z 816.105 and indicates a theoretical frequency selectivity of better than 1 Hz. The mass spectrum recorded after application of this ejection waveform is shown in Fig. 4B and demonstrates that all unwanted ions were successfully removed from the cell. Moreover, comparison of the resolution and the S/N ratio and resolution of the peak at m/z 816.09 before and after isolation indicates that the isolated ions remain unaffected [26,27].

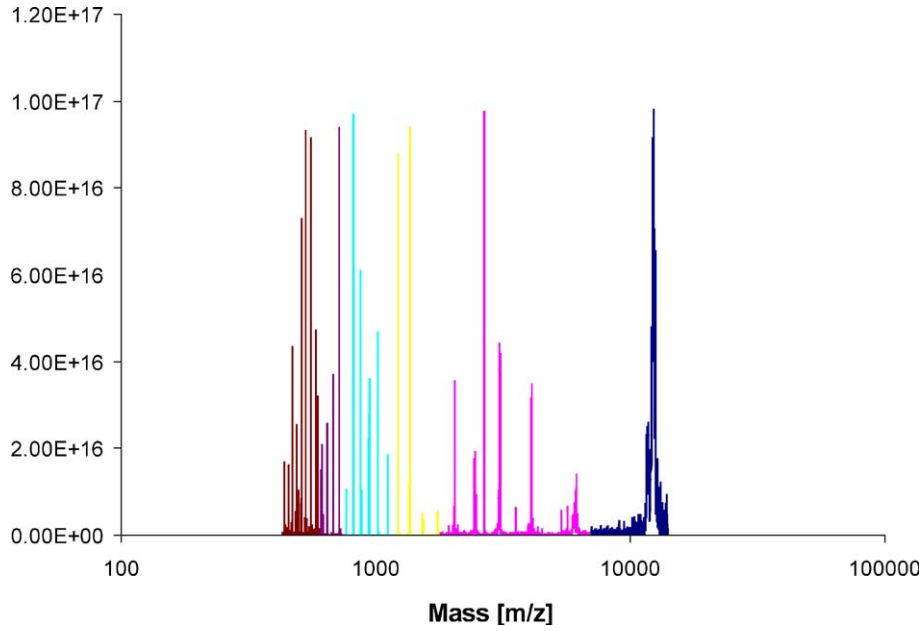

Fig. 8. ESI-FTMS spectrum of Cytochrome C. Peaks grouped by relative abundance and scales adjusted for visibility. Intensity multiplication factors are: 1^+ charge state, 2500X; 2^+ to 6^+, 750X; 7^+ to 10^+, 10X; 11^+ to 16^+, 1X; 17^+ to 20^+, 40X; 21^+ to 28^+, 800X.

The frequency selectivity of the above mentioned SWIFT algorithm was quantified by performing a series of similar experiments in which the center of the notch was shifted in steps of 0.01 μ (corresponding with ∼1.6 Hz) from *m*/*z* 816.045 to *m*/*z* 816.165 as shown in Fig. 5. The signal intensities are plotted against the experiment number, 1 through 18. In these experiments it was observed that a shift of 0.01 u in the center of the notch corresponds to the difference between most efficient isolation and 50% efficient isolation of the *m*/*z* 816.105 peak. We therefore conclude that the frequency selectivity at the boundaries of the isolation notch was approximately 3.2 Hz. The close spacing of the isotope cyclotron frequencies can also be seen in the sudden appearance of the next higher mass isotope at *m*/*z* 816.172.

Heterodyne or "narrowband" measurements can greatly reduce the data load and simultaneously improve signal-to-noise via the digital filtering of data. The new system employs four digital down converters (DDCs) that can each measure a different frequency range defined by the center frequency and a filter bandwidth. All four can be operated simultaneously, as demonstrated in Fig. 6 which shows four separate charge states measured at once on each of the four DDCs. The bandwidth was the same for all four spectra. One range can be measured a very high resolution (high center frequency) while a lower center frequency measures the same bandwidths but a wider mass range.

The new data system has the ability to adjust the level of any parameter within an experiment relative to any other parameter, thereby facilitating tuning and diagnosis of bugs as well as automating measurement, as intended. This configuration requires that the VME memory is dumped to the PC before the parameter is adjusted. This adds a data transfer dead time to the duty cycle of the experiment that is usually acceptable to the user. However, the system retains the ability to store all measurements that fit into the VME crate's memory if control of the parameter being diagnosed is wrested from the software or, as in the case of coupling an HPLC to the source, there is no need to make any sequential changes. Fig. 7 shows a simple example where the bias voltage of the final source quadrupole is ramped slowly from −25 to −0.5 V in steps of 0.5 V while measuring a Cytochrome C distribution. The measured power spectra are shown versus quad bias on the left with an expansion of the 6^+ and 10^+ charge states shown for clarity on the right top and bottom, respectively. The total and selected ion chromatograms for the 2D mass spectra with respect to scan number are shown at the top of each spectrum; these data can be used to optimize the source conditions with respect to this parameter. The experimental set-up turns on the rf of the quadrupoles for 1 s during which ions are transmitted to the cell in the presence of a collision gas, there is a 1 s delay to allow some thermalization of the ions' kinetic energies and the pumpdown of the background collision gas pressure, and the transient duration is 330 ms. The total duration of a single experimental cycle from initialization until the end of the individual measurement defines the duty cycle, in this case ∼2.35 s/cycle or 0.43 Hz. In the absence of the pulsed gas collisional cooling, the data rate is expected to exceed 1 Hz.

Full optimization of the source parameters can be used to extend the measurement dynamic range. Fig. 8 shows an ESI spectrum of the $(M + nH)^{n+}$ Cytochrome C ions for $n = 1$ through [28]. This represents a three orders of magnitude mass range. Wide mass ranges are becoming increasingly important in MS^n studies since highly charged precursors

tend to yield much lower charged products with *m*/*z* values potentially much higher than the precursor and, simultaneously, small fragments that retain much of the precursor charge that can appear drastically lower on the *m*/*z* scale.

4. Summary and conclusions

The design of a novel FTICR-MS system controller has been described. It has been used to perform FTICR-MS experiments in which monoisotopic components from ESI generated polymer distributions and single 15+ charge state isotopes from the ESI generated ion distribution of Cytochrome C have been successfully isolated in the analyzer cell. Based on these measurements the frequency selectivity allowed by the system hardware is measured to be better than 4 Hz. This accuracy is however worse than the resolution in the calculated waveforms (<1 Hz). It is presently believed that this is due to residual off-resonance excitation from the SWIFT pulse itself and not due to frequency instabilities in the AWG hardware. Future experiments based on longer isolation waveforms are envisaged to prove this.

By virtue of the AWG's large memory size and its flexibility in constructing output sequences, the system is ideally suited for complex FTICR-MS experiments such as SWIFT-based two-dimensional mass spectrometry [28], multistage tandem mass spectrometry, and the various hyphenated online forms of mass spectrometry (such as HPLC-FTICR-MS). Its stand-alone operation and easy interfacing make the AWG compatible with virtually any FTICR apparatus.

The conversion to "unlimited" memory has expanded the capabilities by making high-resolution spectra achievable in the broadband experiment. This is especially important in wide mass range measurements that would exceed the bandwidth imposed in a simple heterodyne experiment, as well as in MS/MS and ECD experiments where the product ions can easily exceed this same bandwidth limit.

The system has proven capable of unchaperoned automation by changing the values of the outputs relative to a scan number or another input value. The next step is to implement data dependent automation which will allow implementation of simple iterative tools to genetic algorithms for automated tuning and data collection.

Acknowledgements

We would like to acknowledge P.B O'Connor and L.A. McDonnell for useful discussion in realisation of this instrument. This work is part of the research program no. 49 "Mass spectrometric imaging and structural analysis of biomacromolecules" of the "Stichting voor Fundamenteel Onderzoek der Materie (FOM)", which is financially supported by the "Nederlandse organisatie voor Wetenschappelijk Onderzoek (NWO)".

References

[1] M.B. Comisarow, A.G. Marshall, Chem. Phys. Lett. 26 (1974) 489.
[2] M.B. Comisarow, A.G. Marshall, Chem. Phys. Lett. 25 (1974) 282.
[3] A.G. Marshall, S.H. Guan, Phys. Scr. T59 (1995) 155.
[4] A.G. Marshall, C.L. Hendrickson, G.S. Jackson, Mass Spectrom. Rev. 17 (1998) 1.
[5] D.W. Mitchell, R.D. Smith, J. Mass Spectrom. 31 (1996) 771.
[6] P.B. Grosshans, P.J. Shields, A.G. Marshall, J. Chem. Phys. 94 (1991) 53412.
[7] S.C. Beu, D.A. Laude, Anal. Chem. 63 (1991) 22003.
[8] M.A. Freitas, E. King, S.D.H. Shi, Rapid Commun. Mass Spectrom. 17 (2003) 363.
[9] R.T. McIver, Y.Z. Li, R.L. Hunter, Abstracts of Papers of the American Chemical Society 1997, p. 213, 215-ANYL.
[10] M.W. Senko, J.D. Canterbury, S.H. Guan, A.G. Marshall, Rapid Commun. Mass Spectrom. 10 (1996) 18394.
[11] F.M. White, J.A. Marto, A.G. Marshall, Rapid Commun. Mass Spectrom. 10 (1996) 18459.
[12] A.G. Marshall, T.C.L. Wang, T.L. Ricca, J. Am. Chem. Soc. 107 (1985) 7893.
[13] S. Guan, R.T. McIver, J. Chem. Phys. 92 (1990) 58416.
[14] L. Chen, A.G. Marshall, Rapid Commun. Mass Spectrom. 1 (1987) 39.
[15] L. Chen, T.C.L. Wang, T.L. Ricca, A.G. Marshall, Anal. Chem. 59 (1987) 449.
[16] S.H. Guan, J. Chem. Phys. 93 (1990) 84425.
[17] A.J.R. Heck, L.J. Dekoning, F.A. Pinkse, N.M.M. Nibbering, Rapid Commun. Mass Spectrom. 5 (1991) 406.
[18] J.W. Gauthier, T.R. Trautman, D.B. Jacobson, Anal. Chim. Acta 246 (1991) 211.
[19] L.J. de Koning, N.M.M. Nibbering, S.L. van Orden, F.H. Laukien, Int. J. Mass Spectrom. 165 (1997) 209.
[20] A.J.R. Heck, P.J. Derrick, Anal. Chem. 69 (1997) 36037.
[21] R.M.A. Heeren, K. Vekey, Rapid Commun. Mass Spectrom. 12 (1998) 11751.
[22] L. Drahos, R.M.A. Heeren, C. Collette, E. De Pauw, K. Vekey, J. Mass Spectrom. 34 (1999) 13739.
[23] X.H. Guo, M.C. Duursma, A. Al-Khalili, R.M.A. Heeren, Int. J. Mass Spectrom. 225 (2003) 71.
[24] X.H. Guo, M.C. Duursma, A. Al-Khalili, L.A. McDonnell, R.M.A. Heeren, Int. J. Mass Spectrom. 231 (2004) 37.
[25] J.B. Fenn, M. Mann, C.K. Meng, S.F. Wong, C.M. Whitehouse, Science 246 (1989) 64.
[26] P.B. O'Connor, F.W. McLafferty, J. Am. Soc. Mass Spectrom. 6 (1995) 533.
[27] P.B. O'Connor, D.P. Little, F.W. McLafferty, Anal. Chem. 68 (1996) 542.
[28] C.W. Ross, S.H. Guan, P.B. Grosshans, T.L. Ricca, A.G. Marshall, J. Am. Chem. Soc. 115 (1993) 78541.